

1 **Molecular remodeling in *Populus PdKOR* RNAi roots profiled using LC-MS/MS proteomics**

2

3 **Paul E. Abraham<sup>1</sup>, Anna Matthiadis<sup>2</sup>, Robert L. Hettich<sup>1</sup> and Udaya C Kalluri<sup>2\*</sup>**

4 \*Corresponding Author; kalluriudayc@ornl.gov

5 Author affiliation: Chemical Sciences Division<sup>1</sup> and Biosciences Division<sup>2</sup>, Oak Ridge National  
6 Laboratory, PO BOX 2008, Oak Ridge, TN 37831-6422

7

8 *This manuscript has been authored by UT-Battelle, LLC under Contract No. DE-AC05-  
9 00OR22725 with the U.S. Department of Energy. The United States Government retains and the  
10 publisher, by accepting the article for publication, acknowledges that the United States  
11 Government retains a non-exclusive, paid-up, irrevocable, world-wide license to publish or  
12 reproduce the published form of this manuscript, or allow others to do so, for United States  
13 Government purposes. The Department of Energy will provide public access to these results of  
14 federally sponsored research in accordance with the DOE Public Access  
15 Plan(<http://energy.gov/downloads/doe-public-access-plan>).*

16

17 **Abstract**

18 Plant endo- $\beta$ -1,4-glucanases belonging to the Glycoside Hydrolase Family 9 have functional roles  
19 in cell wall biosynthesis and remodeling via endohydrolysis of (1 $\rightarrow$ 4)- $\beta$ -D-glucosidic linkages.  
20 Modification of cell wall chemistry via RNAi-mediated downregulation of *Populus deltoides*  
21 *KOR1* (*PdKOR*), a endo- $\beta$ -1,4-glucanase gene, in *Populus deltoides* has been shown to have  
22 functional consequences for the composition of secondary metabolome and the ability of modified  
23 roots to interact with beneficial microbes. The molecular remodeling that underlies the observed  
24 differences at metabolic, physiological, and morphological levels in roots is not well understood.  
25 Here we used a LC-MS/MS-based proteome profiling approach to survey the molecular  
26 remodeling in root tissues of *PdKOR* and control plants. A total of 14316 peptides were identified  
27 and these mapped to 7139 *P. deltoides* proteins. Based on 90% sequence identity, the measured  
28 protein accessions represent 1187 functional protein groups. Analysis of GO categories and

## Dataset Brief

29 specific individual proteins showed differential expression of proteins relevant to plant-microbe  
30 interactions, cell wall chemistry, and metabolism. The new proteome dataset serves as a useful  
31 resource for deriving new hypotheses and empirical testing pertaining to functional roles of  
32 proteins and pathways in differential priming of plant roots to interactions with microbes.

33 A greater understanding of the functional implications of plant biomass chemistry optimization  
34 efforts and the underlying molecular remodeling is critical to closing the knowledge gaps in  
35 sustainable bioenergy crop development. We have previously reported that RNAi-mediated down-  
36 regulation of the *Populus deltoides KOR* (*PdKOR1*) gene, belonging to the endo- $\beta$ -1,4-glucanase  
37 family, results in altered cell wall, secondary metabolome and associated microbiome composition  
38 [1,2]. Greenhouse co-culture studies showed that interactions with beneficial microbes were  
39 impacted as a result of the gene modification. Here, we summarize results from the first proteomics  
40 characterization of roots from *PdKOR* and control plants grown in the greenhouse.

41 Greenwood stem cuttings were rooted and grown in ProMix potting soil at 25°C temperature under  
42 long day length (16 h) regime in the greenhouse. At the end of five weeks of growth, roots from  
43 three biological replicates of *PdKOR* RNAi and control (empty vector transformed) lines were  
44 destructively harvested, bulk roots were rinsed in water and blotted dry, and fine roots were  
45 collected in 15 mL tubes, flash-frozen in liquid nitrogen, and store at -80°C. To effectively extract  
46 and recover proteins from roots, we employed a combination of physical and chemical lysis  
47 procedures previously described, albeit with minor modifications [3]. Root samples were ground  
48 to powder using a Qiagen TissueLyser II adapter pre-cooled to -80°C at a frequency of 30 for 20  
49 seconds and suspended in lysis buffer (4% SDS in 100 mM NH<sub>4</sub>HCO<sub>3</sub>), boiled for 5 min, sonically  
50 disrupted (30% amplitude, 10 s pulse with 10 s rest, 2 min total pulse time), and then boiled for an  
51 additional 5 min. The crude protein extract was pre-cleared via centrifugation and proteins were  
52 precipitated using a chloroform/methanol/water extraction procedure. Dried protein pellets were  
53 resuspended in 2% SDC (100 mM NH<sub>4</sub>HCO<sub>3</sub>) and protein amounts were estimated by performing  
54 a BCA assay (Pierce biotechnology). For each sample, an aliquot of ~100 ug of protein was  
55 digested via two separate additions of sequencing-grade trypsin (Promega, 1:75 [w:w]), once  
56 overnight followed by another for 3 hr. at 37 °C. The peptide mixture was adjusted to 1% formic  
57 acid to precipitate Sodium deoxycholate (SDC). Hydrated ethyl acetate was added to each sample  
58 at a 1:1 [v:v] ratio three times to effectively remove SDC. Samples were then placed in a SpeedVac

## Dataset Brief

59 Concentrator (Thermo Fischer Scientific) to remove ethyl acetate and further concentrate the  
60 sample. The peptide-enriched flow-through was quantified by BCA assay, desalted on RP-C18  
61 stage tips (Pierce Biotechnology), and then stored at -80°C.

62 Sample peptide mixtures were analyzed on a Q-Exactive Plus mass spectrometer (Thermo Fischer  
63 Scientific) coupled with a with a Proxeon EASY-nLC 1200 liquid chromatography (LC) pump  
64 (Thermo Fisher Scientific) as previously described with some minor modifications [4]. In brief,  
65 peptides were separated on a 75  $\mu$ m inner diameter microcapillary column packed with 50 cm of  
66 Kinetex C18 resin (1.7  $\mu$ m, 100  $\text{\AA}$ , Phenomenex) placed in a column heater (Sonation GmbH) at  
67 60°C. For each sample, a 2  $\mu$ g aliquot was loaded in buffer A (0.1% formic acid, 2% acetonitrile)  
68 and eluted with a linear 150 min gradient of 2 – 20% of buffer B (0.1% formic acid, 80%  
69 acetonitrile), followed by an increase in buffer B to 30% for 10 min, another increase to 50% buffer  
70 for 10 min and concluding with a 10 min wash at 98% buffer A. The flow rate was kept at 200  
71 nL/min. MS data was acquired with the Thermo Xcalibur software version 4.27.19 using the a  
72 top10 data-dependent acquisition strategy using a resolution of 70,000 at m/z 200. A 1.6 m/z  
73 isolation window and fragmentation of precursor ions was performed by higher-energy C-trap  
74 dissociation (HCD) with a normalized collision energy of 30 eV. MS/MS sans were performed at  
75 a resolution of 17,500 at m/z 200.

76

77 MS raw data files were searched against the *Populus deltoides* reference proteome database  
78 (<https://phytozome.jgi.doe.gov/pz/portal.html>) to which common contaminant proteins had been  
79 added. A decoy database, consisting of the reversed sequences of the target database, was  
80 appended in order to establish the false-discovery rate (FDR) at the spectral level. For standard  
81 database searching, the peptide fragmentation spectra (MS/MS) were analyzed by Proteome  
82 Discoverer v2.3. The MS/MS were searched using the MS Amanda v2.0 [5] and was configured  
83 to derive fully tryptic peptides using settings for high-high MS/MS data: MS1 mass tolerance of 5  
84 ppm and MS2 mass tolerance of 0.02 Da. A static modification on cysteines (iodoacetamide;  
85 +57.0214 Da), a dynamic modification on methionine (oxidation; 15.9949) and aspartate and  
86 glutamate (methylation; 14.016) were considered. The results were processed by Percolator [6] to  
87 estimate q values. Peptide spectrum matches (PSMs) and peptides were considered identified at a  
88 q value <0.01 (Supplemental Table 1).

89

## Dataset Brief

90 For label-free quantification, MS1-level precursor intensities (peak areas) were derived from the  
91 Minora Feature and Precursor ions quantifier nodes using default parameters. Protein abundance  
92 values were Log2-transformed and normalized using InfernoRDN v1.1 [7] by LOESS across  
93 biological replicates and median centering adjustments across the global dataset. Missing values  
94 were imputed (low abundance resampling method) using Perseus [8]. A Student's t-test and a  
95 permutation-based FDR was implemented to characterize protein abundance differences between  
96 *PdKOR1* and control roots. Differential protein abundances having a q-value of 0.05 and a Log2  
97 difference of 1 were considered significantly different and were further investigated (Supplemental  
98 Table 2). Whole-genome gene ontology (GO) term annotation was performed using Blast2GO [9]  
99 with a blastp E-value hit filter of  $1 \times 10^{-5}$ , an annotation cutoff value of 55 and a GO weight of 5.  
100 Using ClueGO, [10] observed GO biological processes were subjected to the right-sided  
101 hypergeometric enrichment test at default settings and p-value correction was performed using the  
102 Holm-Bonferroni step-down method. Minimal reporting of functional groups was achieved by  
103 implementing ClueGO GO term fusion and grouping settings were selected to reduce GO term  
104 redundancy. The term enriched at the highest level of significance was used as the representative  
105 term for each functional cluster. The GO terms at adjusted  $p < 0.05$  were considered significantly  
106 enriched (Supplemental Table 3). Additionally, the *P. deltoides* proteome was annotated by  
107 Mercator4 v2.0 to analyze protein function in MapMan v3.6 [11]. A Wilcoxon Rank Sum Test  
108 was performed and identified functional bins that exhibit a differential abundance behavior  
109 (Supplemental Table 4) that corroborates the GO enrichment analysis.

110  
111 Overall, LC-MS/MS proteomic characterization of *PdKOR* and control roots (Figure 1a) revealed  
112 a comparable total/ average number of proteins identified from each sample group (triplicates of  
113 *PdKOR* or control). Principle Component Analysis (PCA) differentiated the replicates into their  
114 respective groups. This dataset provides the first insight into significantly differential proteome  
115 expression between *PdKOR* and control roots (Figure 1b). Key classes of plant proteins with  
116 potential role in mediating plant-microbe interactions; Receptor-like serine/threonine-protein  
117 kinases, calcium signaling components, cell wall biosynthesis enzymes and peroxidases, were  
118 observed to be differentially expressed at the protein level.

119 Proteome data analysis based on GO classifications and relative expression levels of specific  
120 protein isoforms suggests molecular remodeling in *Populus PdKOR* RNAi roots relative the

121 control. Our data shows differential expression of homologs of common symbiosis pathway (CSP)  
122 factors. CSP has been shown to be core to mediation of rhizobia-legume, actinorhizal and  
123 arbuscular mycorrhizal symbiosis and includes calcium signaling factors, such as calcium-  
124 dependent protein kinase (CDPK) [12] and Calcium and calmodulin-dependent protein kinase  
125 (CCaMK) [13], and in transmembrane signal transduction such as LYK3 receptor-like kinases  
126 (Lysin motif receptor-like kinases (LysM RLKs). Homologs in distinct plant species, *Lotus*  
127 *japonicus* [14] *Medicago truncatula* [15], have been shown to be involved in beneficial nodule-  
128 forming microbes.

129 Disease resistance proteins, abscisic acid receptors and heat shock proteins belonging to biotic and  
130 abiotic stress responsive pathways, show a 4-5-fold higher expression in *PdKOR* roots. The  
131 differential expression of proteins in lignin biosynthesis and phenylpropanoid pathways, such as  
132 cinnamoyl-CoA reductase, laccase, UDP-glucose flavonoid 3-O-glucosyltransferase 6 and  
133 Flavonol 3-O-glucosyltransferase ascorbate peroxidase, as well as in primary sugar and  
134 carbohydrate metabolism pathways as shown by differential GO term enrichment is supported by  
135 the differential lignin, secondary metabolite and sugar levels reported previously from *PdKOR* and  
136 control plants [1]. Differential expression of specific cell wall biosynthesis pathway genes and  
137 disease resistance response proteins has also been reported in a study to identify core  
138 transcriptional response to inoculation of three different ectomycorrhizal fungi on oak tree roots  
139 [16]. Homolog of one such key core upregulated factor, myo-inositol oxygenase (MIOX) [17], is  
140 differentially expressed in *PdKOR* roots.

141 In summary, the extensive LC-MS/MS proteomics dataset provides insights into global changes  
142 in root proteome as a consequence of modification of a cell wall remodeling gene, *PdKOR*, in *P.*  
143 *deltoides*. Previous findings on phenotypic implications of *PdKOR* gene modification on *Populus*  
144 cell wall chemistry, secondary metabolome and interactions with microbes are supported [1, 2], in  
145 part, by the proteome remodeling shown here by differential proteome analysis. Further functional  
146 analysis of targeted proteins, across cellular to whole plant contexts, is needed to validate the  
147 hypothesized functional consequences of the differentially expressed proteins.

148

149 **Acknowledgments**

150 This research was sponsored by the Genomic Science Program, U.S. Department of Energy, Office  
151 of Science, Biological and Environmental Research, as part of the Plant Microbe Interfaces  
152 Scientific Focus Area at Oak Ridge National Laboratory (<http://pmi.ornl.gov>). Oak Ridge National  
153 Laboratory is managed by UT-Battelle, LLC, for the U.S. Department of Energy under contract  
154 DE-AC05-00OR22725.

155

156 **Keywords**

157 Cell wall chemistry, proteome, plant-microbe interaction, *PdKOR*, host, root

158 **Conflicts of Interest**

159 The authors declare no conflicts of interest.

160

161 **Data deposition in open access database:** All spectral data collected in this study was deposited  
162 at the ProteomeXchange Consortium via the MASSIVE repository. The project identifier is  
163 MSV000085068 and the data can be reviewed under the username “MSV000085068\_reviewer”  
164 and password “PdKOR”. [is private mode until manuscript is under review]

165

166 **References**

- 167 1. U.C. Kalluri, R.S. Payyavula, J. L. Labb  , N. Engle, G. Bali, S.S. Jawdy, R.W. Sykes, M.  
168 Davis, A. Ragauskas, G.A. Tuskan, T.J. Tschaplinski, *Front Plant Sci.* **2016**, 7, 1455.
- 169 2. A.M. Veach, D. Yip, N.L. Engle, Z.K. Yang, A. Bible, J. Morrell-Falvey, T.J. Tschaplinski,  
170 U.C. Kalluri, C.W. Schadt, *Plant and Soil.* **2018**, 429, 349.
- 171 3. P. Abraham, R.J. Giannone, R.M. Adams, U. Kalluri, G.A. Tuskan, R.L. Hettich, *Mol Cell  
172 Proteomics.* **2013**, 12, 106.

173

176 4. M.I. Villalobos Solis, R.J. Giannone, R.L. Hettich, P.E. Abraham, *Anal. Chem.* **2019**, *91*,  
177 7273-7279.

178

179 5. V. Dorfer, P. Pichler, T. Stranzl, J. Stadlmann, T. Taus, S. Winkler, K. Mechtler, MS  
180 Amanda, *J. Proteome Res.* **2014**, *13*, 3679.

181

182 6. L. Käll, J.D. Canterbury, J. Weston, W.S. Noble, M.J. MacCoss, *Nat. Methods.* **2007**, *4*,  
183 923.

184

185 7. A.D. Polpitiya, W.J. Qian, N.Jaitly, V.A. Petyuk, J.N. Adkins, D.G. Camp II, G.A.  
186 Anderson, R.D. Smith, **2008**, *24*, 1556.

187

188 8. S. Tyanova, T. Temu, P. Sinitcyn, A. Carlson, M.Y. Hein, T. Geiger, M. Mann, J. Cox,  
189 *Nat Methods* **2016**, *13*, 731.

190

191 9. A. Conesa, S. Gotz, J.M. Garcia-Gomez, J. Terol, M. Talon, M. Robles, *Bioinformatics*  
192 **2005**, *21*, 3674.

193

194 10. G. Bindea, B. Mlecnik, H. Hackl, P. Charoentong, M. Tosolini, A. Kirilovsky, W.H.  
195 Fridman, F. Pages, Z. Trajannoski, J. Galon, *Bioinformatics* **2009**, *25*, 1091.

196

197 11. R. Schwacke, G. Y. Ponce-Soto, K. Krause, A. M. Bolger, B. Arsova, A. Hallab, K.  
198 Gruden, M. Stitt, M. E. Bolger, B. Usadel, *Mol Plant* **2019**, *12*, 879.

199

200 12. N. Takeda, T. Maekawa, M. Hayashi, *The Plant Cell*, **2012**, *24*, 810.

201

202 13. B.J. Sieberer, M. Chabaud, J. Fournier, A.C.J. Timmers, D.G. Barker, *The Plant J.* **2012**,  
203 69, 822.

204

205 14. E.B. Madsen, L.H. Madsen, S. Radutoiu, M. Olbryt, M. Rakwalska, K. Szczyglowski, S.  
206 Sato, T. Kaneko, S. Tabata, N.J. Sandal, J. Stougaard, *Nature*. **2003**, *425*, 637.

207

208 15. E. Limpens, C. Franken, P. Smit, J. Willemse, T. Bisseling, R. Geurts. *Science*. **2003**, *302*,  
209 630.

210

211 16. M.L. Bouffaud, S. Herrmann, M.T. Tarkka, M. Bonn, L. Feldhahn, and F. Buscot, *BMC*  
212 *Genomics* **2020**, *21*.

213

214 17. U. Kanter, B. Usadel, F. Guerineau, Y. Li, M. Pauly, and R. Tenhaken, *Planta* **2005**, *221*,  
215 243.

216

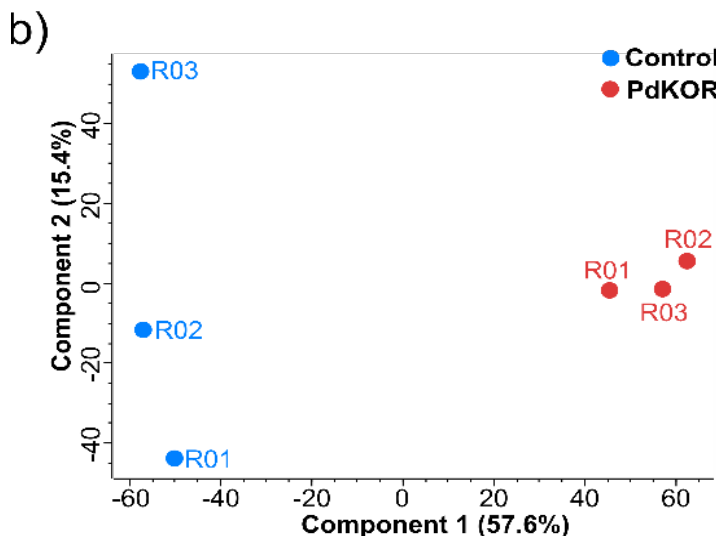
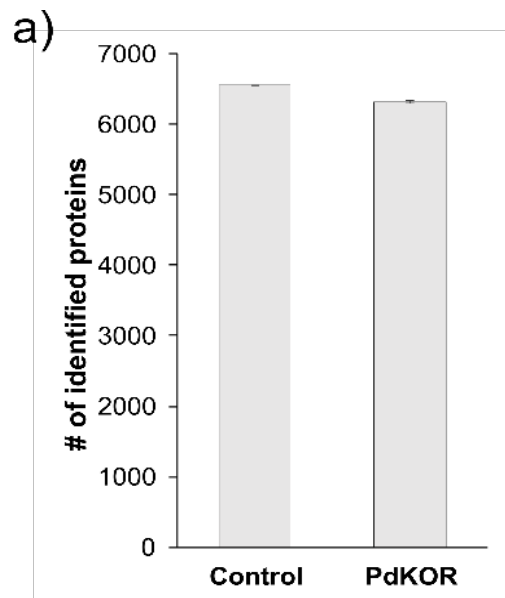
217

218

219

220

221



222

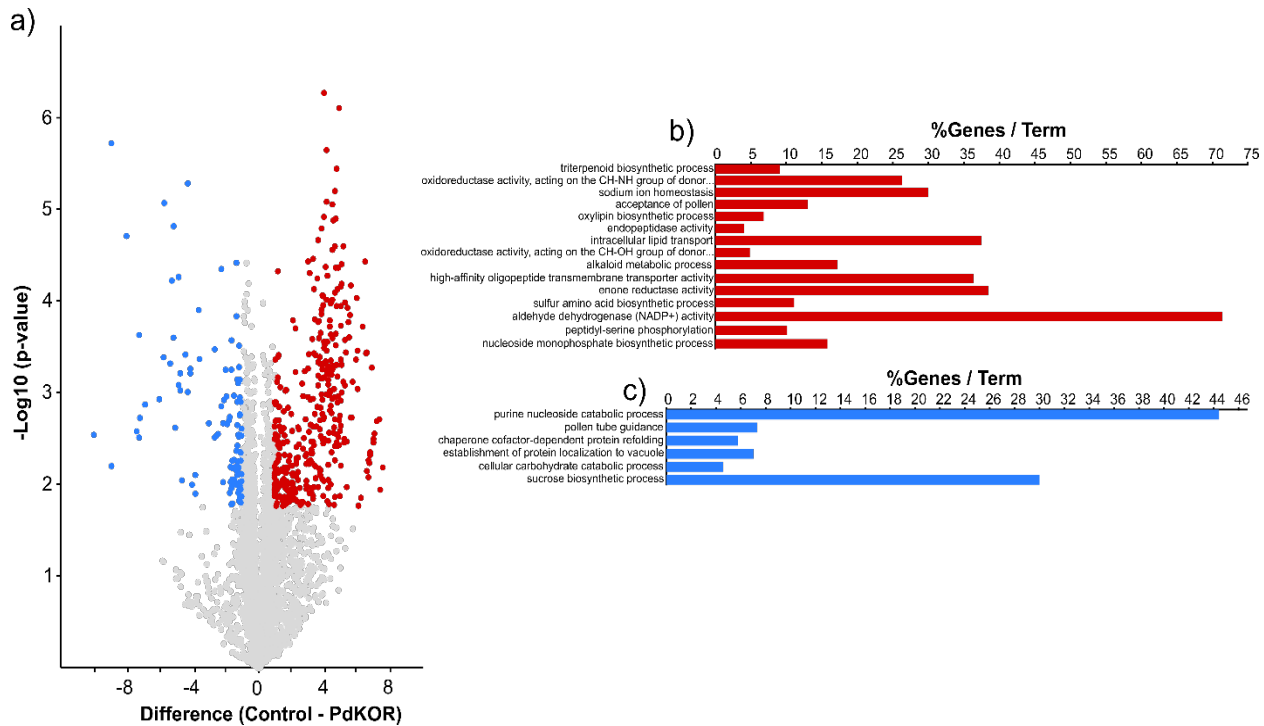
223

224

225 **Figure 1.** a) Average number of identified proteins for each sample group. Error bars represent the  
226 standard deviation across biological triplicates. b) Plot illustrating results from principal  
227 component analysis (PCA).

228

229



230

231

232

**Figure 2:** a) Volcano plot illustrating differential Log2 protein abundances. Significant differences were determined by a Student's t-test followed by a permutation-based FDR calculation. Gene ontology (GO) term enrichment was performed (right-sided hypergeometric enrichment test and p-value correction was performed using the Holm-Bonferroni step-down method) to identify biological processes enriched in proteins more abundant in the b) control and c) *PdKOR*. GO term fusion and grouping settings were selected to reduce GO term redundancy and the term enriched at the highest level of significance was used as the representative term for each functional cluster. The GO terms at adjusted  $p < 0.05$  were considered significantly enriched. Red and blue correspond to an increase or decrease, respectively, in the relative protein abundance in Control when compared to the abundance value in *PdKOR* lines.

243

244

245

246

247 **Supplemental Table 1.** Filtered results (< 1% FDR) of peptides and their associated *P. deltoides*  
248 protein accessions.

249

250 **Supplemental Table 2.** List of identified proteins and their relative abundances, which are  
251 represented as normalized Log2-transformed values. Missing values were replaced by random  
252 numbers drawn from a distribution optimized to simulate a typical abundance region near the limit-  
253 of-detection. A Student's t-test was performed, and permutation-based FDR was implemented.  
254 Protein abundance differences with p-values > 0.05 and Log2 differences >1 were considered  
255 significantly different.

256

257 **Supplemental Table 3.** Summary of results from ClueGO gene ontology enrichment test.

258

259 **Supplemental Table 4.** Summary of results from Wilcoxon Rank sum test performed by MapMan  
260 v3.6.